Invited Paper

Resonant Field Enhancement in Hybrid Plasmonic Geometries

Xinchao Lu [1*, 2], Li Wang [2], Weili Zhang [1]

[1] School of Electrical and Computer Engineering, Oklahoma State University,
Stillwater, Oklahoma 74078, USA

[2] Beijing National Laboratory for Condensed Matter Physics, Institute of Physics, Chinese
Academy of Sciences, PO Box 603, Beijing 100190, People's Republic of China

[*1] E-mail: xinchao@iphy.ac.cn

Abstract: We report an anomalous field enhancement of terahertz transmission in metallic, hybrid plasmonic geometries. The integration of a rectangle particle in the hole not only results in an eight times normalized transmittance compared to that of the hole-only counterpart, but also tailors polarization-dependent transmission discrepancy encountered in arrays of rectangular holes. In addition, plasmonic structures made of metallic rings integrated into the subwavelength holes are investigated. The emergence and the interplay of various resonances sustained by the hybrid plasmonic samples are elucidated. To reveal a coherent physical picture, relevant dimensions of the samples are modified and their impact on the resonance properties is analyzed. The understanding of the interplay of various resonances will foster applications which require plasmonic substrates to exhibit simultaneously resonances at well-defined frequencies and line widths.

1. Introduction

Surface plasmon has captured the extensive attention due to their potential in a wide range of applications, such as near-field microscopy, spectroscopy, and integrated photonic devices. It is widely accepted that both the enhanced transmission through perforated metal film and the field enhancement within subwavelength structures are mediated with surface plasmon excitation. Three mechanisms are essential to understand the resonance of surface plasmon. The first is the dipole localized surface plasmon (DLSP) sustained by the resonance of metallic particle, and the scattered fields are related to the shape, size and substrate matrix of the particles. Complementary, holes integrated into the metallic film will also introduce resonance. The excitation of localized surface plasmon (LSP) modes in a single hole that are patterned into the metallic film usually leads to a transmission resonance close to the cut-off frequency of the guided wave [1-2], which challenges the transmission predicted by Bethe [3]. The third mechanism is the excitation of propagating surface plasmon (SP) at the metal-dielectric interface of the periodic hole array drilled into the metallic film. Based on the enhanced transmission through the periodic hole array, it has been reported that further enhancement can be achieved by employing complex plasmonic structures, such as corrugating metallic periodic grooves surrounding a single hole [4], placing metamaterial structures at the near field of the hole [5-6], or using circular coaxial structures [7], [8-14]. Although, these resonances are individually well understood, their combined action remains largely unexplored but promises to greatly affect the peculiar details of the resonances.

Meanwhile, although the high dielectric constant of metal at low frequencies brings weak surface plasmon confinement to the metal surface, the artificial structures on the metal film can introduce "spoof" surface plasmon. As a result, the excitation of surface plasmon at terahertz frequencies can be tailored by the metallic structures. Here, we present terahertz transmission enhancement through two hybrid structures, e.g. hole array integrated with rectangle particles and rings. Compared with hole-only array, hybrid array demonstrates the presence of more transmission enhancement. Terahertz time-domain spectroscopy (THz-TDS) measurements and numerical analysis supported by analytical considerations illustrate the physical mechanisms of the more enhanced transmission sustained by the hybrid structures [15-17].

2. Sample fabrication

Using photolithography and metallization processes, we fabricate the hybrid arrays with 190 *nm*-thick aluminum film on a silicon substrate (0.64 *mm* thick, n-type resistivity ρ = 12 Ω *cm*). Figure 1 illustrates a microscopic image of three hybrid arrays. In figure 1(a) and 1(c), the dimension of the holes is fixed as 100×80 *μm^2* with same periodicity 160 *μm*. The hole-rectangle sample has dimensions of 80×40 *μm^2* for the rectangle particle; while ring sample has dimensions of $80 \times 60 / 60 \times 40$ *μm^2* for the inner ring. Figure 1(b) shows the nonperiodic array with same hybrid structure in figure 1(a).
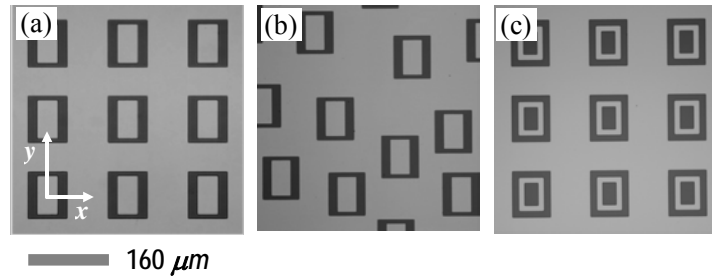
Fig. 1 Microscopic image of three hybrid arrays. The dimension of the holes is fixed as 100×80 *μm^2*. (a) Periodic hole-rectangle hybrid array with 80×40 *μm^2* for the rectangle particle, periodicity 160 *μm*. (b) Nonperiodic hole-ring hybrid array with same hybrid structure in (a). (c) Periodic hole-ring hybrid array with $80 \times 60 / 60 \times 40$ *μm^2* for the inner ring, periodicity 160 *μm*.

3. Experiment results and analysis

Figure 2 shows frequency-dependent amplitude transmissions of the hole-rectangle hybrid and the counterpart hole-only array. The data were recorded by terahertz time-domain spectroscopy (THz-TDS) under normal incident radiation with electric field parallel to the longer axis of the structure, $E \parallel y$ [15, 18]. It is interesting to note that the measured transmission of the hole-rectangle hybrid exhibits a significant increase over that of the hole-only array at the Si-Al [±1, 0] mode. In addition, the resonance frequency of the hole-rectangle hybrid reveals noticeable red-shift.
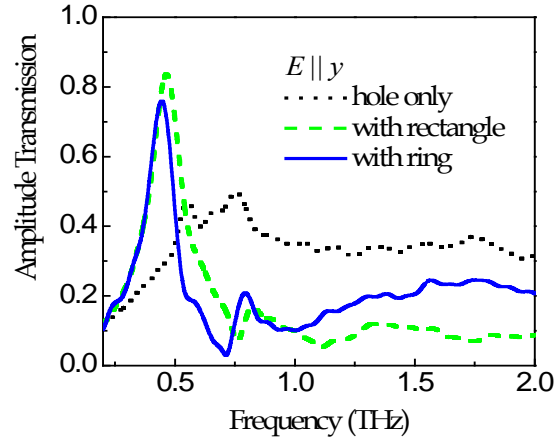
Fig. 2 Measured frequency-dependent spectra of hole-rectangle hybrid with $100 \times 80 \ \mu m^2$ holes and $80 \times 60 \ \mu m^2$ inner particles (dash curve) and the hole-only counterpart (dotted curve), with periodicity $160 \ \mu m$ and $E \parallel y$.

Such resonant properties are systematically characterized in a series of hole-rectangle hybrid structures with various dimensions of inner particles, but fixed periodicity and dimensions of holes. Figure 3(a) shows the peak amplitude transmission and normalized transmittance as functions of particle length (along y axis) obtained from measurements and numerical calculations using Finite Integration Technique. The normalized transmittance is evaluated by normalizing the transmitted power to the geometrical area of the aperture. The particle length shows an extensive influence on the field enhancement when the particle width (along x axis) is fixed at $60 \ \mu m$. The calculated amplitude transmission at the Si-Al $[\pm 1,0]$ mode approaches its maximum at length $70 \ \mu m$, while the normalized transmittance (over the open area of the coaxial) experiences a monotonic increasing. The measured normalized transmittance reveals a value of 5.64 at length $80 \ \mu m$, which is eight times of that in the hole-only counterpart, showing a good consistency with the calculation. In Fig. 3(b) we show that the resonance red-shifts with increasing length of the particles. The observed transmission properties of the hole-rectangle hybrid structures are essentially a result of resonant excitations of DLSPs of the particles and their coupling with SPs, LSPs of the holes, and direct scattering. The increased particle length along electric field strengthens its DLSP resonance, which gives rise to resonance enhancement and red-shift through coupling with SPs and LSPs of the holes [17, 19]. The effect of direct scattering is also revealed from Fig. 2, where the non-resonant background of the hole-rectangle hybrid structure is noticeably reduced compared to that of the hole-only array due to modification of direct scattering by the addition of the particle.
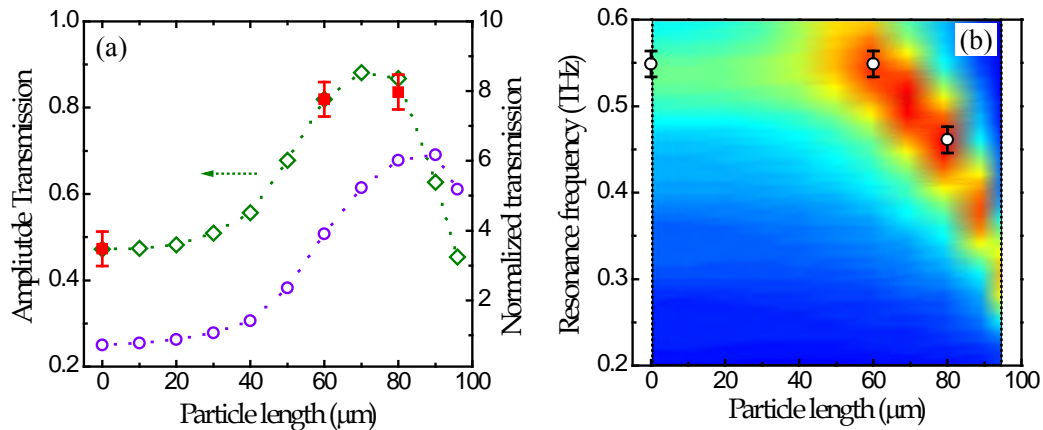
Fig. 3 (a) Simulated peak amplitude transmission (diamonds) and normalized transmittance (circles) as a function of the length of inner particles (*y* axis). The squares manifest the measured peak amplitude transmission. (b) Simulated resonance frequency as a function of the length of inner particles. The hollow circles are the experimental resonance frequencies, $E \parallel y$.

Figure 4(b) shows the measured amplitude transmission with terahertz electric field switched to $E \parallel x$. As expected, the hole-only array exhibits much stronger peak transmission (0.85) than that of $E \parallel y$ due to polarization dependent nature of the rotationally asymmetric holes [18]. When the $80 \times 40 \ \mu m^2$ particle is integrated in the hole, unlike the $E \parallel y$ orientation, no obvious modification is observed in the amplitude transmission. It is interesting to note that the extensive polarization dependent transmission discrepancy in the rectangular holes is very well compensated by DLSPs of the integrated particles through coupling with SPs and LSPs in the hole-rectangle hybrid. For example, the measured peak amplitude transmissions in the hole-rectangle hybrid with the $80 \times 60 \ \mu m^2$ inner particles for $E \parallel y$ and $E \parallel x$ are 0.84 and 0.88, respectively, while the values are 0.47 and 0.85 for the hole-only array. As shown in Fig. 4(a), for $E \parallel y$, the minor difference in the transmissions between the periodic and nonperiodic arrays indicates that SPs play a less important role than DLSPs of particles and LSPs of the holes. However, the drastically reduced transmission in the nonperiodic array, as shown in Fig. 4(b), also reveals that SPs play an important role in the transmission field enhancement at $E \parallel x$.
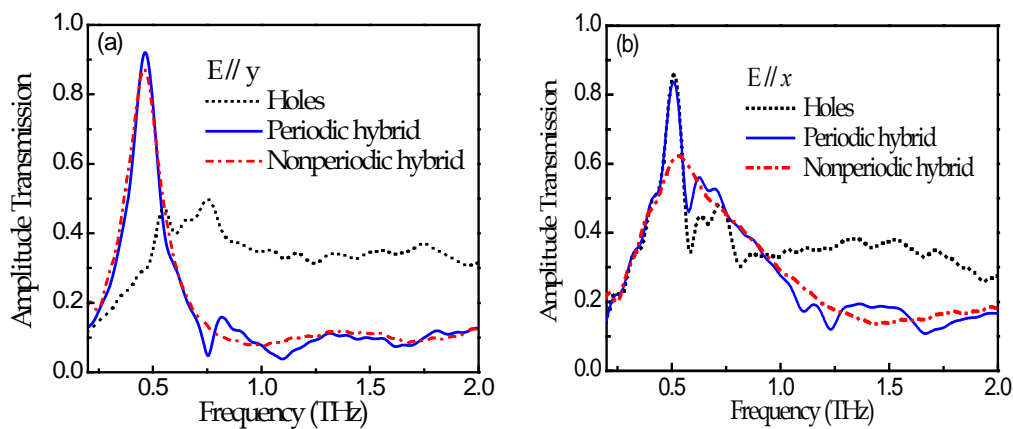
Fig. 4 Measured frequency-dependent spectra of periodic hole-rectangle hybrid (solid curve) and nonperiodic (dash-dotted curve) hybrid with $100 \times 80 \ \mu m^2$ holes and $80 \times 40 \ \mu m^2$ inner particles and the hole-only counterpart (dotted curve), with periodicity $160 \ \mu m$ with (a) $E \parallel y$, (b) $E \parallel x$.

The asymmetric resonance line shape of the coaxial geometries is analyzed by use of the Fano model, which describes the interaction between the discrete resonant state and the continuum scattering state [7, 17, 20-23]. Here, contributions to the discrete resonant state include DLSPs of the particles, SPs, and LSPs of the holes. The Fano transmittance can be written as

$$I_{Fano} = I_a + I_b \left(1 + \sum_v \frac{q_v}{\Delta \varepsilon_v} \right)^2 \Bigg/ \left[1 + \left(\sum_v \frac{1}{\Delta \varepsilon_v} \right)^2 \right], \text{ where } \Delta \varepsilon_v = (\omega - \omega_v)/(\Gamma_v/2), \quad I_a \text{ is a slowly varying}$$

transmittance, I_b is the continuum transmittance coefficient that couples with the discrete resonant states, $\omega_v/2\pi$ is resonance frequency, $\Gamma_v/2\pi$ is linewidth, and q_v is the Breit-Wigner-Fano coupling coefficient for the vth discrete state. As shown in Fig. 5(a), the experimental transmittance of the coaxial array with the $80 \times 40\ \mu m^2$ inner particles and $E \parallel y$ is well fit by the Fano model, indicating that both Al-Si [±1,0] and [±1,±1] resonances are resulted from the contributions of DLSPs of the particles, SPs, LSPs of the holes, and the direct scattering.

In Fig. 5(b), we show the measured angle-resolved transmission spectra of the same hole-rectangle hybrid at $E \parallel y$. The Al-Si [±1,0] mode at 0.46 *THz* exhibits angle-independent behavior due to an dominant contribution of DLSPs of the particles. The high frequency Al-Si [±1,±1] mode near 0.80 *THz*, however, experiences resonance splitting with incident angle greater than 10°, owing to a weak effect of DLSPs, but a primary contribution of the SP resonance. Based on the angle-resolved experiment, we further characterize the coupling mechanism between different states of the hole-rectangle hybrid by use of a Hamiltonian, $\hat{H} = \hat{H}_1 + \hat{H}_2 + \hat{H}_3 + \hat{V}$, where the eigenstates $\hat{H}_1$, $\hat{H}_2$, and $\hat{H}_3$ stand for the DLSP resonance of the particle, the Al-Si SP [−1,0] mode, and the contributions of both LSP of the hole and direct scattering [22], respectively, and $\hat{V}$ is the coupling term between these eigenstates represented by coupling coefficients κ_{12}, κ_{13}, and κ_{23}. The corresponding eigen frequencies, $\omega_1/2\pi$ and $\omega_2/2\pi$ are the DLSP and SP resonance frequencies, respectively, given by their dispersion relations [17, 22], and $\omega_3/2\pi$ is resulted from both LSPs of the holes and direct scattering [22]. The variables, i.e. ω_3, κ_{12}, κ_{13}, and κ_{23} are obtained by diagonalizing $\hat{H}$ using the angle-resolved transmission data in fig. 5(b). At $E \parallel y$, the calculated coefficients are $|\kappa_{12}| = 8.03 \times 10^{-3}$, $|\kappa_{13}| = 0.103$, and $|\kappa_{23}| = 9.70 \times 10^{-3}$, indicating that the coupling between DLSPs and LSPs primarily contributes to the field enhancement, which further explains the angel-independent behavior of the Al-Si [±1,0] mode observed in Fig. 5(b). In addition, this is consistent with the measured amplitude transmission of a nonperiodic counterpart array composed of same number density of coaxial, as shown in Fig. 4(a). At $E \parallel x$, the calculated coefficients are $|\kappa_{12}| = 0.151$, $|\kappa_{13}| = 5.00 \times 10^{-4}$, and $|\kappa_{23}| = 2.35 \times 10^{-2}$, manifesting the dominant role of the coupling between DLSPs and SPs. The drastically reduced transmission in the nonperiodic array, as shown in Fig. 4(b), also reveals that SPs play an important role in the transmission field enhancement at $E \parallel x$.
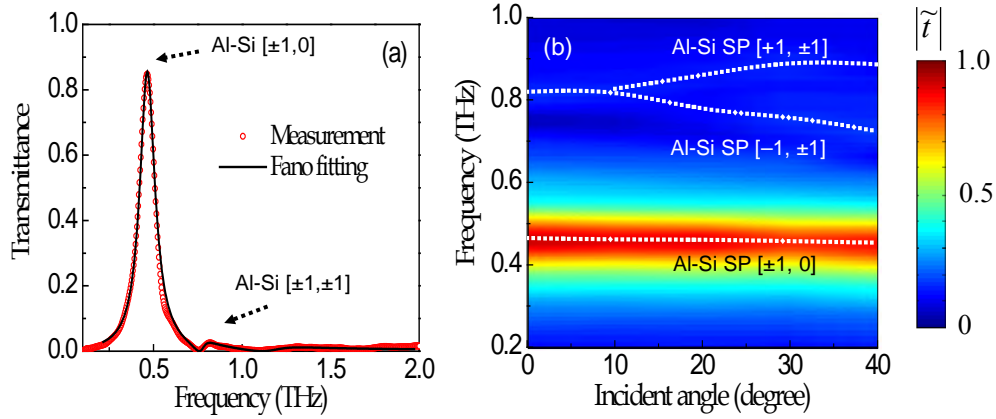
Fig. 5 (a) Measured (open circles) and Fano fit (solid curve) transmittance of the coaxials with inner particle $80 \times 40 \ \mu m^2$, periodicity 160 μm, and $E \parallel y$. The fitting parameters are $I_a = 0$; $I_b = 0.0013$; $q_1 = 24.5$; $\Gamma_1/2\pi = 0.11$; $\omega_1/2\pi = 0.4485$; $q_2 = 1.35$; $\Gamma_2/2\pi = 0.07$; $\omega_2/2\pi = 0.7680$; $q_3 = 1.8323$; $\Gamma_3/2\pi = 0.25$; $\omega_3/2\pi = 1.1852$. (b) Measured angle-resolved transmission of the same coaxial array at $E \parallel y$. The dashed curves represent the resonance modes.

Integrating metallic particles into the holes will add the spectra of a particle plasmon resonance to the transmission spectra of the periodic hole array and enhances the transmission when compared to the hole array alone in certain spectral intervals. However, the emerging resonance line width of such a hybrid structure is limited by the line width of the particle plasmon. This resonance tends to be rather broad since the electrical dipolar resonance of the metallic particle can couple nicely to the incident field. This causes radiative losses to be large; leading to the rather broad resonance. This is detrimental for many applications and such problem needs to be solved. A general approach would be the use of ring like particles instead of their solid counterparts. Radiative losses are known to be strongly reduced and they promise to have therefore a much narrower line width. Here we analyze the plasmonic response of such a hybrid geometry composed of a hole and a ring that are coaxially integrated in a unit cell.

In figure 2, although the ring itself exhibits a stronger resonance with a narrower line width when compared to the solid rectangle, the amplitude transmission of the hole-ring composite is slightly reduced than that of the hole-rectangle array. Compared to the solid rectangle, the narrower resonance line width of the ring is a manifestation of suppressed radiative coupling, leading to a larger life time of the resonance and a lower damping [24]. Correspondingly, the hole-ring composite possesses less damping and thus narrower transmission line width. The slightly lower transmission is furthermore an indication of lower excitation strength of the resonance which comes along with the enhanced life time. Both properties reflect that the field distribution of the resonance is less electric-dipolar like which would have been coupled much better to free space radiation. Also, the resonance is red-shifted since the inner and the outer surface forming the ring do couple [19]. This leads to a hybridization of the plasmon modes excited at the inner and the outer surface for which the symmetric (antisymmetric) mode is red- (blue-) shifted. However, only the symmetric mode is excitable because of symmetry constraints imposed by the system and the illumination; therefore only the red-shifted resonance persists.

To further investigate the hybrid structures, we fix the dimension of the hole to be 80×100 μm^2 and observe the influence of the ring geometry on the transmission. The inset of Fig. 6(a)

shows for referential purpose the transmission properties of samples made of rings only. In this sample we fixed the outer dimensions of $80 \times 60 \ \mu m^2$ and also fixed the inner length 60 μm. By modifying inner width from 20 to 40 μm, the transmission in resonance decreases and the resonance frequency is red-shifted. This is fully in-line with the expected red-shift since the coupling between the inner and outer surfaces of the ring is enforced. Figure 6(a) shows the transmission properties of hybridized structure with the same rings with $E \parallel y$. With inner width increasing from 20 to 40 μm, the amplitude transmission decreases slightly from 0.79 to 0.76, and the resonance frequency experiences a red-shift. Since the gap between the ring and the hole is fixed, a major modification of the coupling conditions between the ring and hole can be excluded. The similarities of the resonance shift between the ring-only and the hole-ring samples suggest the same physical origin as outlined above for the ring alone. The slightly decrease in the amplitude transmission manifests the same physical mechanism as the reduced amplitude transmission of the hole-ring structure compared with hole-rectangle sample, as mentioned before. Meanwhile, by fixing the inner edge on the other hand, the outer dimension of the ring also modifies the resonance of the hybrid structure. In Fig. 6(b), the inner dimension of the ring is fixed to be $40 \times 20 \ \mu m^2$, and outer length increases from 60 to 80 μm with the same outer width to be 40 μm, the resonance frequency experiences obvious red-shift from 0.55 to 0.46 THz. The enhanced coupling strength between the ring and the hole lowers the frequency of the hybrid resonance.

By having the same hole dimensions, we also investigate the coupling effect between the ring and hole with a fixed wire width of the inner ring. The ring structures are designed as $80 \times 60 \ \mu m^2 / 60 \times 40 \ \mu m^2$, $70 \times 50 \ \mu m^2 / 50 \times 30 \ \mu m^2$, and $60 \times 40 \ \mu m^2 / 40 \times 20 \ \mu m^2$ (outer / inner dimension) to keep the same wire width be 10 μm with a varying gap to be 10, 15, and 20 μm, respectively. The transmission spectra are shown in Fig. 6(c). With increasing ring dimensions, i.e. a smaller gap, the coupling between the ring and hole gets stronger and more plasmons couple with the direct transmission, which introduces more transmission potentially. However, the line width of the resonance becomes narrower, which indicates less radiative damping. The enhanced plasmon life time suppresses the radiation and brings reduced transmission. As a result, the amplitude transmission is the balance between the coupling and the radiative decay. In Fig. 6(c), although the coupling is stronger, the amplitude transmission at gap being 10 μm diminished. The maximum amplitude transmission is obtained at gap to be 15 μm. Also, the stronger coupling forced by the lower gap sizes shifts the resonance frequency towards smaller values.

To achieve more quantitative insights into the coupling strength among the hole and ring with altering dimensions of the rings, we introduce the Hamiltonian, $\hat{H} = \hat{H}_1 + \hat{H}_2 + \hat{V}$, where the eigenstates $\hat{H}_1$ and $\hat{H}_2$ stand for the lowest resonance modes of the ring-only and hole-only arrays, respectively, and $\hat{V}$ is the coupling term between these eigenstates. The calculated coupling coefficient $|\kappa_{12}|^2$ with various ring dimensions is shown in Fig. 6(d). When outer length is fixed as 80 μm, i.e. the gap between the hole and ring is maintained as 10 μm, the change of inner dimension influences $|\kappa_{12}|^2$ quite marginal due to the weak modification of the charge distribution induced along the outer edge of the ring. With the gap varying from 10 to 20 μm, $|\kappa_{12}|^2$ experiences an extensive reduction from 8.0×10^{-3} down to 1.0×10^{-3}. It indicates that the outer length of the ring along the E field which relates to the gap between the hole and ring dominates the coupling effect.
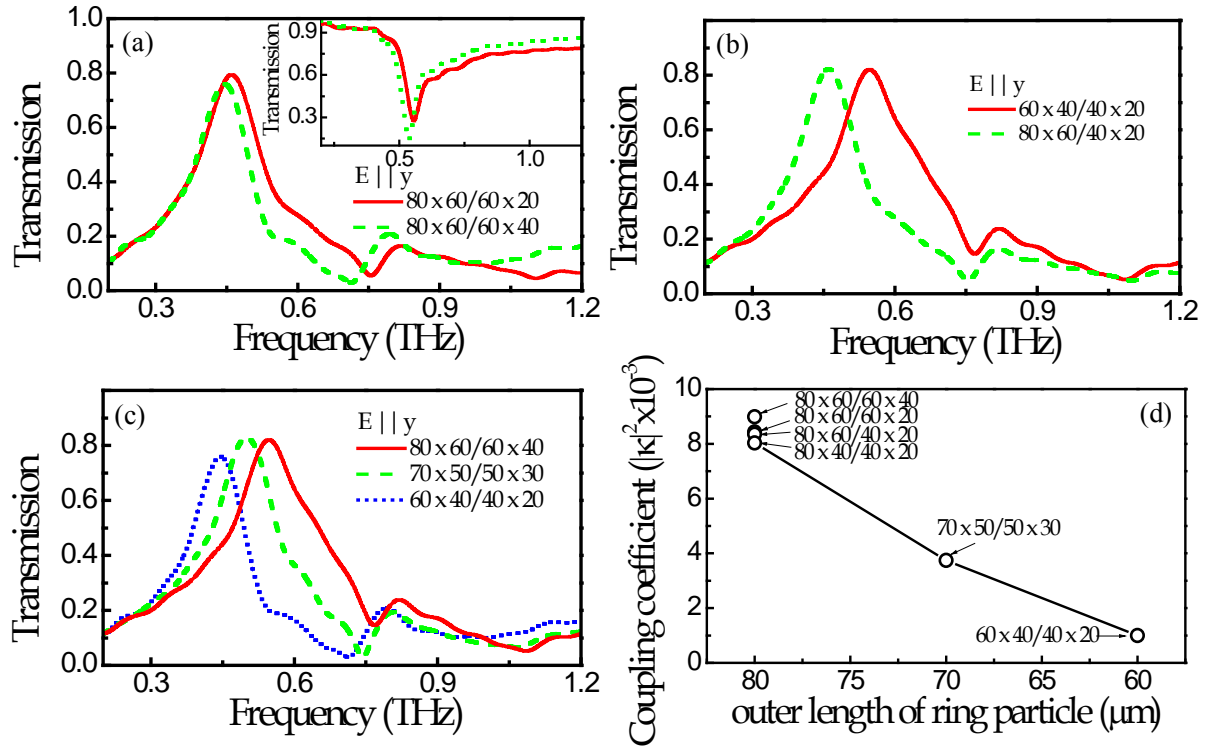
Fig. 6 (a) Peak amplitude transmission as a function of the dimension of ring particle, the holes are fixed as 100 × 80 μm^2 with periodicity 160 μm. Fix outer length = 80 μm, outer width = 60 μm, inner length = 60 μm, inner width = 20 (solid curve) and 40 μm (dash dot curve), respectively, with $E \parallel y$. Inset: peak amplitude transmission of ring particles only array. (b) Fix the inner dimension as inner length = 40 μm, inner width = 20 μm, outer dimensions are 60 × 40 (solid curve), and 80 × 60 (dash curve) μm^2, respectively, with $E \parallel y$. (c) Fix the ring width = 10 μm, the dimension of ring particles are 80 × 60 / 60 × 40 μm^2 (dot curve), 70 × 50 / 50 × 30 μm^2 (dash dot curve), and 60 × 40 / 40 × 20 μm^2 (solid curve), which corresponds to gap = 10, 15, and 20 μm, respectively, with $E \parallel y$. (d) Calculated coupling coefficient as a function of different ring particle dimension, $E \parallel y$.

Although the normalized transmittance increases with stronger coupling coefficient when the gap between the hole and ring changes, the normalized transmittance and coupling coefficient exhibit an inverse proportion with a fixed gap. The coupling coefficient $|\kappa_{12}|^2$ and normalized transmittance of the hole-ring arrays with fixed outer ring dimension 80 × 60 μm^2, i.e. both gaps between the hole and ring are unaltered, are listed in Tab. 1. With a fixed gap, the modified coupling coefficient can be predominantly linked to the modified spectral properties of the ring. It can be clearly seen in Tab. 1 that the less the size of the inner ring, the larger the coupling strength. The less ring size indicates the less radiative decay rate of plasmons, which is proportional to the total number of electrons oscillating [17]. It can be stated that for the larger coupling strength, the line width of the resonance is narrower that indicates a longer life time. We also note that the normalized transmittance is reduced simultaneously with a larger coupling strength. This is an indication that the field distribution of the resonance looses its dipolar character when the coupling is increased and the external field, which is an electric dipolar field, cannot couple sufficiently well to the structure and the resonance is excited with a lower strength. This enhances the quality factor of the resonance and causes the line width to be reduced; but lowers seemingly the normalized transmittance. The analysis agrees well with the experiment results shown in Fig. 6(a).

Tab. 1 Calculated coupling coefficients and normalized transmittance for the hybrid structures with various dimensions of the inner ring, but fixed hole-ring gap to be 10 μm along both x and y direction.

Outer/Inner dimensions (μm^2)	80×60/60×40	80×60/60×20	80×60/40×20
Coupling Coefficient ($\lvert\kappa\rvert^2 \times 10^3$)	8.99	8.43	8.35
Normalized Transmittance	4.62	5.04	5.40

4. Conclusions

In conclusion, we investigated terahertz properties of plasmonic crystals made of periodic rectangular holes hybridized with rectangles and rings, respectively. The impact of geometrical dimensions of the rectangles within hole-rectangle hybrid structure is systematically exploited, which shows that a number of factors contribute to the observed field enhancement, including DLSPs of the particles, SPs, LSPs of the hole, and direct scattering. Meanwhile, by fixing the dimension of the holes, both the outer and inner dimensions of the rings were found to influence the resonance behavior of the hole-ring hybrid structure. The outer dimension of the ring predominantly modifies the gap between the ring and hole and influence the coupling strength between them, which plays a dominant role in the resonance shift. The inner dimension of the ring makes a little effect on the frequency shift, line width, which can be used to fine resonance tuning of sensors. Also, both coupling strength and the radiative decay of the hybrid structure determine the normalized transmittance, which can be improved by selecting optimized gap and ring size. Such hybrid plasmonic structures would be potentially used for terahertz sensing applications.

References

[1] F. J. García-Vidal, E. Moreno, J. A. Porto, and L. Martín-Moreno, "Transmission of Light through a Single Rectangular Hole", *Phys. Rev. Lett.*, 95, 103901-4, (2005).

[2] C. Rockstuhl, T. Zentgraf, T. P. Meyrath, H. Giessen, F. Lederer, "Resonances in complementary metamaterials and nanoapertures.", *Opt. Express*, 16, 2080-2090, (2008).

[3] H. A. Bethe, "Theory of Diffraction by Small Holes.", *Phys. Rev.*, 66, 163-182, (1944).

[4] H. J. Lezec, A. Degiron, E. Devaux, R. A. Linke, L. Martín-Moreno, F. J. García-Vidal, and T. W. Ebbesen, "Beaming Light from a Subwavelength Hole", *Science*, 297, 820-822, (2002).

[5] A. Alu, F. Bilotti, E. Nader, and L. Vegni, "Metamaterial covers over a small hole", *IEEE Trans. Antenn. Propag.*, 54, 1632-1643, (2006).

[6] K. Aydin, A. O. Cakmak, L. Sahin, Z. Li, F. Bilotti, L. Vegni, and E. Ozbay, "Split-Ring-Resonator-Coupled

Enhanced Transmission through a Single Subwavelength Hole", *Phys. Rev. Lett*., 102, 013904-4, (2009).

[7] W. Fan, S. Zhang, B. Minhas, J. M. Kevin, and S. R. J. Brueck, "Enhanced Infrared Transmission through Subwavelength Coaxial Metallic Arrays", *Phys. Rev. Lett*., 94, 033902-4, (2005).

[8] A. Moreau, G. Granet, F. Baida, and D. Van Labeke, "Light transmission by subwavelength square coaxial hole arrays in metallic films", *Opt. Express*, 11, 1131-1136, (2003).

[9] W. Jia and X. Liu, "Mechanism of the superenhanced light transmission through 2D subwavelength coaxial hole arrays", *Phys. Lett*. A, 344, 451-456, (2005).

[10] Y. Poujet, J. Salvi, and F.I. Baida, "90% extraordinary optical transmission in the visible range through annular hole metallic arrays", *Opt. Lett*., 32, 2942-2944, (2007).

[11] S. M. Orbons, M. I. Haftel, C. Schlockermann, D. Freeman, M. Milicevic, T. J. Davis, B. Luther-Davies, D. N. Jamieson, and A. Roberts, "Dual resonance mechanisms facilitating enhanced optical transmission in coaxial waveguide arrays", *Opt. Lett*., 33, 821-823, (2008).

[12] S. Wu, Q. Wang, X. Yin, J. Li, D. Zhu, S. Liu, and Y. Zhu, "Enhanced optical transmission: Role of the localized surface plasmon", *Appl. Phys. Lett*., 93, 101113-3, (2008).

[13] A. A. Yanik, X. Wang, S. Erramilli, M. K. Hong, and H. Altug, "Extraordinary midinfrared transmission of rectangular coaxial nanohole arrays", *Appl. Phys. Lett.*, 93, 081104-3, (2008).

[14] M.J. Kofke, D. H. Waldeck, Z.Fakhraai, S. Ip, and G. C. Walker, "The effect of periodicity on the extraordinary optical transmission of annular hole arrays", *Appl. Phys. Lett*., 94, 023104-3, (2009).

[15] D. Grischkowsky, S. Keiding, M. van Exter, and Ch. Fattinger, "Far-infrared time-domain spectroscopy with terahertz beams of dielectrics and semiconductors", *J. Opt. Soc. Am. B*, 7, 2006-2015, (1990).

[16] M. He, A. K. Azad, S. Ye, and W. Zhang, "Far-infrared signature of animal tissues characterized by terahertz time-domain spectroscopy", *Optics Commun*., 259, 389-392, (2006).

[17] X. Lu, J. Han, and W. Zhang, "Resonant terahertz reflection of periodic arrays of subwavelength metallic rectangles", *Appl. Phys. Lett*., 92, 121103-3, (2008).

[18] D. Qu, D. Grischkowsky, and W. Zhang, "Terahertz transmission properties of thin, subwavelength metallic holearrays", *Opt. Lett*., 29, 896-898, (2004).

[19] X. Lu and W. Zhang, "Terahertz localized plasmonic properties of subwavelength ring and coaxial geometries", *Appl. Phys. Lett*., 94, 181106-3, (2009).

[20] U. Fano, "Effects of Configuration Interaction on Intensities and Phase Shifts", *Phys. Rev*., 124, 1866-1878, (1961).

[21] C. Genet, M. P. van Exter, and J. P. Woerdman, "Fano-type interpretation of red shifts and red tails in hole array transmission spectra", *Optics Comm*., 225, 331-336, (2003).

[22] J. Han, A. K. Azad, M. Gong, X. Lu, and W. Zhang, "Coupling between surface plasmons and nonresonant transmission in subwavelength holes at terahertz frequencies", *Appl. Phys. Lett.*, 91, 071122-3, (2007).

[23] W. Zhang, A. K. Azad, J. Han, J. Xu, J. Chen, and X.-C. Zhang, "Direct Observation of a Transition of a Surface Plasmon Resonance from a Photonic Crystal Effect", *Phys. Rev. Lett*., 98, 183901-4, (2007).

[24] Dahmen, C. and G. von Plessen, "Optical Effects of Metallic Nanoparticles", *Aust. J. Chem*., 60, 447-456, (2007).